A color phase shift profilometry for the fabric defect detection*

SONG Li-mei (宋丽梅)[1]**, **LI Zong-yan** (李宗艳)[1], **CHANG Yu-lan** (常玉兰)[1], **XING Guang-xin** (邢广鑫)[1], **WANG Peng-qiang** (王朋强)[1], **XI Jiang-tao** (习江涛)[2], and **ZHU Teng-da** (朱腾达)[1]

1. Key Laboratory of Advanced Electrical Engineering and Energy Technology, Tianjin Polytechnic University, Tianjin 300387, China

2. School of Electrical, Computer and Telecommunications Engineering, University of Wollongong, Keiraville 2500, Australia

(Received 18 April 2014)

For fabric defect identification in the textile industry, a three-dimensional (3D) color phase shift profilometry (CPSP) method is proposed. The detecting system is mainly composed of one CCD camera and one digital-light-processing (DLP) projector. Before detection, the system should be calibrated to make sure the camera parameters. The CPSP color grating is projected to the measured fabric by DLP projector, and then it is collected by CCD camera to obtain the grating phase. The 3D measurement can be completed by the grating phase difference. In image acquisition, only invariable grating is projected to the object. In order to eliminate the interference from background light during the image acquisition, the brightness correction method is researched for improving the detection accuracy. The experimental results show that the false rate of detecting the fabric defects is 5.78%, the correct rates of detecting the fabric defects of hole and qualified fabric are both 100%, and the correct rates of detecting the fabric defect of scratch and fold are 98% and 96%, respectively. The experiment proves that the proposed method can accurately identify fabric defects.

Document code: A **Article ID:** 1673-1905(2014)04-0308-5

DOI 10.1007/s11801-014-4065-z

Quality control is very important in textile industry. The apparent quality testing of textiles is widely researched in recent years[1], especially the online fabric defects detection. Fabric defects can be generated in all processes of production and they have a wide variety of colors, patterns and classifications. Therefore, it is difficult to detect fabric defects. Currently, most fabric defect detections are based on the analysis and study of two-dimensional (2D) image processing. Henry Y. T. Ngan[2] presents a study of using ellipsoidal decision regions for motif-based patterned fabric defect detection. K. L. Mak[3] proposed a novel defect detection scheme based on morphological filters to tackle the problem of automated defect detection for woven fabrics. Based on adaptive discrete wavelet transform, Yang[4] proposed a method which can identify characteristic distortion mixed fabric defects. Xu[5] analyzed and processed the gray curve of four common fabric defect images and extracted eigenvalues of the defect images, and then identified the defect type based on back propagation (BP) neural network. Besides these methods, Gabor filter method[6] and wavelet transform method[7,8] are also based on 2D image processing to detect fabric defects. However, these methods still can not solve the following detection problems. It is difficult to solve the image disturbances which are brought by wrinkles, flying catkins and the changes of ambient light and background light. And currently these methods are limited in plain fabric defect detection.

Compared with 2D image, three-dimensional (3D) structure of fabric surface contains more information. In the current 3D measurement methods, the one using structured light projection is the most widely used[9]. Among these methods, phase shift profilometry can achieve the measurement with high accuracy based on multiple projections. However, the measuring speed is low and the real-time measurement can not be achieved. In addition, during the process of conventional gray structured light projection, the measured object can not be moved. Therefore, this method is not suitable for online detection. In order to achieve online detection, a color phase shift profilometry (CPSP) method is proposed in this paper on the basis of the previous research in our laboratory[10,11]. The proposed method can achieve

* This work has been supported by the National Natural Science Foundation of China (Nos.60808020 and 61078041), and the Tianjin Research Program of Application Foundation and Advanced Technology (No.10JCYBJC07200).

** E-mail:lilymay1976@126.com

high-precision 3D reconstruction with only invariable grating. And during the process of projection, the object can be moved. With the proposed method, the speed and accuracy of the 3D reconstruction are improved. And it can be applied to the online fabric defect detection, 3D measurement of moving object and other 3D online measurements in industry.

A typical 3D measurement system based on grating projection is shown in Fig.1. This system is made up of a CCD camera and a DLP projector. During the measuring period, the phase-shifted sinusoidal grating fringe is projected to the measured object by DLP projector. By the modulation of measured object, the changed phase of grating fringe can be obtained. Then according to the related algorithm theory, the height information of the measured object can be got by the phase information.

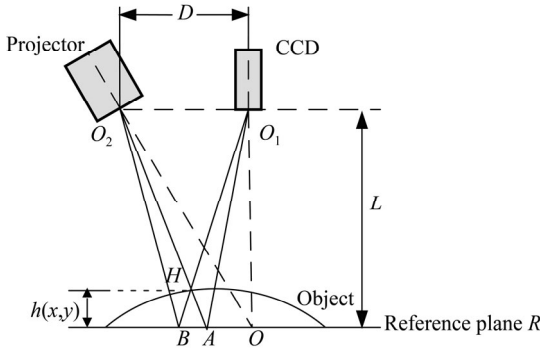

Fig.1 Schematic diagram of the phase shift profilometry

This cross-axis structure is proposed by Takeda. R is the reference plane, H is an arbitrary point on the measured object, the straight line O_1H and the reference plane R intersect at point B, the straight line O_2H and the reference plane R intersect at point A, the height of the point H on the measured object relative to the reference surface is $h(x,y)$, the distance between O_1 or O_2 and the reference surface R is L, and the distance between O_1 and O_2 is D. Parameters L and D can be obtained by calibration.

The incident ray irradiates on point A without the object. After setting the object, the incident ray irradiates on the point H of the object surface. If we observe from the imaging plane, the position of A is equivalent to shifting to the position of B. Thereby, the distance between points A and B, which is expressed as $\overline{AB}$, can carry the height information of the measured object. The phase difference between deformed grating and reference grating is

$$\Delta\varphi(x,y)=2\pi f\overline{AB}, \tag{1}$$

where f is the frequency of the projected sinusoidal grating.

Since the ΔABH and the ΔO_2O_1H are similar, we can obtain

$$\frac{h(x,y)}{L-h(x,y)}=\frac{\overline{AB}}{D}. \tag{2}$$

So from Eqs.(1) and (2), $h(x,y)$ can be expressed as

$$h(x,y)=\frac{L\cdot\Delta\varphi(x,y)}{2\pi fD\pm\Delta\varphi(x,y)}. \tag{3}$$

With CPSP method, three pieces of sinusoidal waveform with a constant phase interval are projected to red, green and blue channels of the color light source respectively at the same time. Fig.2(a), (b) and (c) show the luminance waveforms of red, green and blue channels captured by camera. The brightnesses of sinusoidal waveforms projected to red, green and blue channels respectively can be expressed as

$$I_{\mathrm{R}}(x,y)=b(x,y)\sin[\theta(x,y)], \tag{4}$$

$$I_{\mathrm{G}}(x,y)=b(x,y)\sin[\theta(x,y)+2\pi/3], \tag{5}$$

$$I_{\mathrm{B}}(x,y)=b(x,y)\sin[\theta(x,y)+4\pi/3], \tag{6}$$

where $b(x,y)$ is the luminance modulation information, and $\theta(x,y)$ is the phase of the measured point. During the process of detection, only the color grating shown in Fig.2(d), which is generated by $I_{\mathrm{R}}(x,y)$, $I_{\mathrm{G}}(x,y)$ and $I_{\mathrm{B}}(x,y)$, is projected to the measured object.

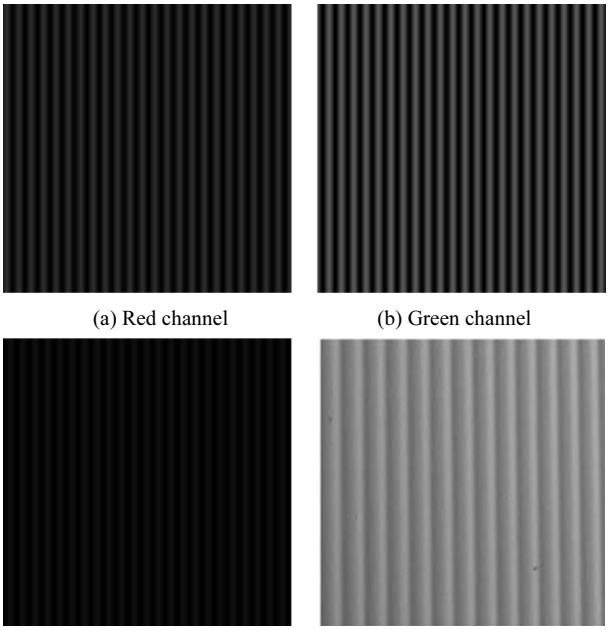

(a) Red channel (b) Green channel

(c) Blue channel (d) Color grating

Fig.2 Optical signal waveforms projected to the red, green, blue channels and the measured object

In the image acquisition process, the brightness information collected by camera and the ideal waveform projected by light are different due to the interference of background light. The brightnesses collected by red, green and blue channels are

$$I_{\mathrm{R}}'(x,y)=a(x,y)+b(x,y)\sin[\theta(x,y)], \tag{7}$$

$$I_{\mathrm{G}}'(x,y)=a(x,y)+b(x,y)\sin[\theta(x,y)+2\pi/3], \tag{8}$$

$$I_{\mathrm{B}}'(x,y)=a(x,y)+b(x,y)\sin[\theta(x,y)+4\pi/3], \tag{9}$$

where $a(x,y)$ is the luminance of background light.

Therefore, the phase of the measured point $\theta(x,y)$ can be calculated by Eqs.(7)–(9) as

$$\theta(x,y)=\arctan\left\{\frac{\sqrt{3}[I_{\mathrm{R}}'(x,y)-I_{\mathrm{B}}'(x,y)]}{2I_{\mathrm{G}}'(x,y)-I_{\mathrm{R}}'(x,y)-I_{\mathrm{B}}'(x,y)}\right\}. \quad (10)$$

In order to extract the height information of the measured object correctly, the discontinuous wrapped phase must be calculated to obtain continuous phase by a certain algorithm. In this paper, the quality guide path algorithm is used for phase unwrapping. The two major problems in quality guide path algorithm are the choice of quality function and the design of unwrapping path.

The second-order difference is selected as quality function for unwrapping, because it can well measure the concavity-convexity of phase. Take 3×3 pixel matrix as an example. As the matrix shown in Fig.3, pixel (i,j) is the central pixel.

$(i-1, j-1)$	$(i, j-1)$	$(i+1, j-1)$
$(i-1, j)$	(i, j)	$(i+1, j)$
$(i-1, j+1)$	$(i, j+1)$	$(i+1, j+1)$

Fig.3 3×3 pixel matrix

Second-order difference $D(i, j)$ containing pixel (i, j) can be expressed as

$$D(i,j)=\sqrt{H^2(i,j)+V^2(i,j)+D_1^2(i,j)+D_2^2(i,j)}\ . \quad (11)$$

In Eq.(9), $H(i, j)$ is the second-order difference value in the transverse direction of (i,j), which is defined as

$$H(i,j)=\gamma[\varphi(i-1,j)-\varphi(i,j)]-\gamma[\varphi(i,j)-\varphi(i+1,j)], \quad (12)$$

$D_1(i,j)$, $V(i,j)$ and $D_2(i,j)$ are the second-order difference values in the first, second and third longitudinal lines of (i, j) matrix, respectively, which are defined as

$$V(i,j)=\gamma[\varphi(i,j-1)-\varphi(i,j)]-\gamma[\varphi(i,j)-\varphi(i,j+1)], \quad (13)$$

$$D_1(i,j)=\gamma[\varphi(i-1,j-1)-\varphi(i,j)]-\gamma[\varphi(i,j)-\varphi(i+1,j+1)], \quad (14)$$

$$D_2(i,j)=\gamma[\varphi(i-1,j+1)-\varphi(i,j)]-\gamma[\varphi(i,j)-\varphi(i+1,j-1)], \quad (15)$$

where γ is the operation of plus or minus $2n\pi$ to make continuous phase of adjacent pixels, and $\varphi(i, j)$ is the phase of pixels (i, j).

As the second-order difference represents concave-convex change, the larger the second-order differential value, the worse the quality of the pixel. Then the quality function $R(i, j)$ can be defined as

$$R(i,j)=\frac{1}{D(i,j)}\ . \quad (16)$$

The descending order of edge quality is selected as the unwrapping path. The edge is the intersection of two pixels in transverse or longitudinal direction. Fig.4(a) shows the pixel quality, and the edge quality can be generated by summing the qualities of two adjacent pixels connected by the edge as shown in Fig.4(b). Edge can be divided into transverse edge and longitudinal edge. The unwrapping path is unrelated to the pixel quality, but has a close connection with edge quality. The unwrapping path should follow descending order of edge quality. These edge qualities are stored in an array according to the values of the qualities.

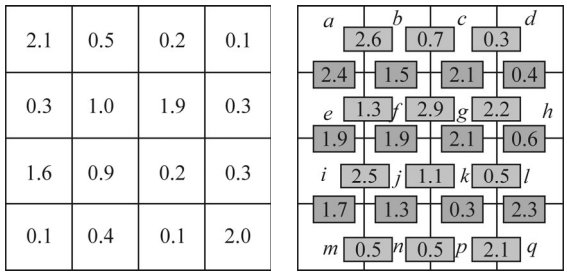

(a) The pixel quality (b) The edge quality

Fig.4 The pixel quality and edge quality

Fig.5 shows the grating phase before and after unwrapping by the quality guide path algorithm. After unwrapping, the phase difference can be obtained with grating phase as shown in Fig.5(b). Then according to Eq.(3), the height information of the object can be got based on the phase difference.

As the luminance responses of three channels are different, amplitudes of brightness collected by the three channels are also different. Therefore, in order to obtain a better effect of 3D reconstruction, the method of brightness correction is researched. The actual brightness distributions collected by the three channels are shown in Fig.6.

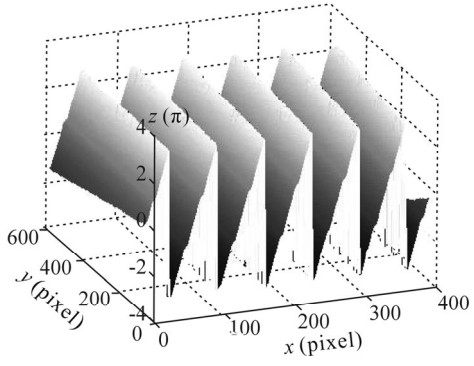

(a) Before unwrapping

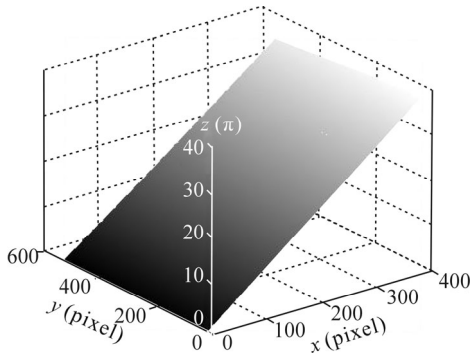

(b) After unwrapping

Fig.5 The grating phases before and after unwrapping

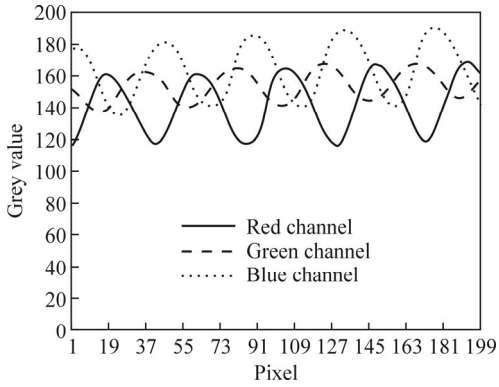

Fig.6 The actual brightness distribution collected by three channels

For the three channels, the luminance response of green channel is the largest usually. Therefore, the optical signal of green channel can be used as a reference to correct the luminance. Assume the image resolution is $W \cdot H$, and the average brightnesses of green, red and blue channels on y axis are Ave_G, Ave_R and Ave_B, respectively, which can be expressed as

$$Ave_G = \frac{\sum_{x=0}^{W}\sum_{y=0}^{H} I_G'(x,y)}{W \cdot H}, \tag{17}$$

$$Ave_R = \frac{\sum_{x=0}^{W}\sum_{y=0}^{H} I_R'(x,y)}{W \cdot H}, \tag{18}$$

$$Ave_B = \frac{\sum_{x=0}^{W}\sum_{y=0}^{H} I_B'(x,y)}{W \cdot H}. \tag{19}$$

Using the average brightness, the brightnesses of the three channels can be normalized. Therefore, the phase of the measured point of $\theta(x,y)$ can be calculated by

$$\theta(x,y) = \arctan\left[\frac{\sqrt{3}(I_R \times \frac{Ave_G}{Ave_R} - I_B \times \frac{Ave_G}{Ave_B})}{2I_G - I_R \times \frac{Ave_G}{Ave_R} - I_B \times \frac{Ave_G}{Ave_B}}\right]. \tag{20}$$

The brightness distribution after brightness correction is shown in Fig.7, and it can be seen that the precision of 3D reconstruction can be improved greatly.

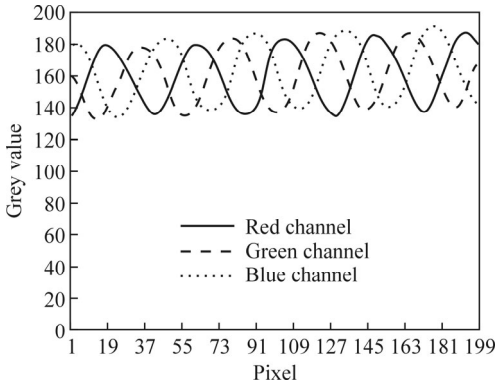

Fig.7 The brightness distribution after brightness correction

In order to validate the effect of the proposed CPSP method in fabric defect detection, seven representative categories of fabric defects are selected as samples for experiment. The number of every category samples is 50, and the number of qualified samples is 50. A total of 400 samples are selected for experiment. The experimental results are shown in Tab.1. And 3D characteristics of fabric defects obtained by the CPSP method are shown in Fig.8.

Tab.1 Defect recognition results

Recognition result / Type	Hole	Broken end	Broken picks	Misend	Mispick	Scratch	Fold	Qualified fabric	Correct rate
Hole	50	0	0	0	0	0	0	0	100%
Broken end	0	45	0	2	0	0	0	3	90%
Broken picks	0	0	44	0	4	0	0	2	88%
Misend	0	4	0	45	0	0	0	1	90%
Mispick	0	0	2	0	46	0	0	2	92%
Scratch	0	0	0	0	0	49	1	0	98%
Fold	0	0	0	0	0	2	48	0	96%
Qualified fabric	0	0	0	0	0	0	0	50	100%

(a) Fold

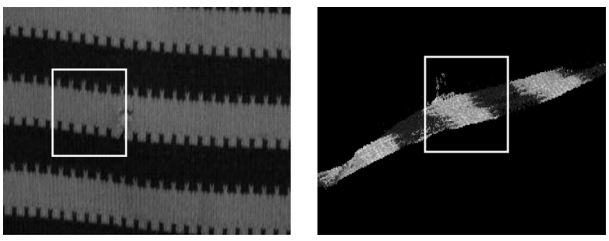

(b) Hold

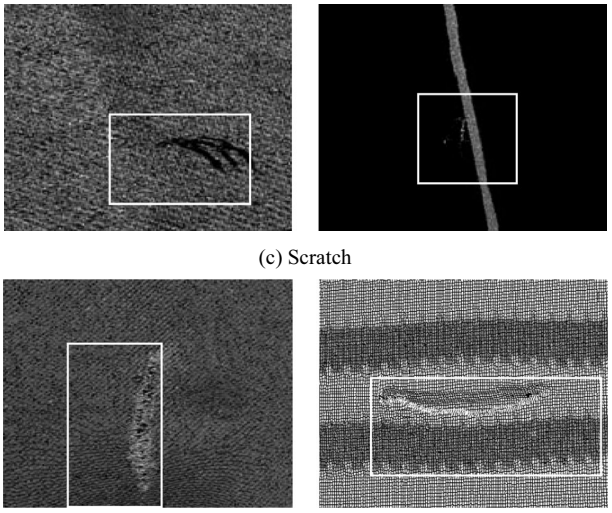

(c) Scratch

(d) Broken end and Broken picks

Fig.8 3D characteristics of fabric defects

There are 23 misclassifications in 400 samples. The false rate of detecting the fabric defects is 5.78%. As shown in Tab.1, the correct rates of detecting the fabric defects of hole and qualified fabric are 100%, and the correct rate of detecting the fabric defect of scratch is 98%. However, for broken end, broken picks, misend and mispick, the recognition accuracies are not so high due to the restriction of similar 3D structure of these fabric defects. But the correct rate of detecting the fabric defect of fold is up to 96%. Compared with 2D detection method, the proposed method can identify the non-defect interference more accurately.

The CPSP method, which is a new 3D optoelectronic measurement method, is proposed in this paper. The CPSP method can achieve high-precision 3D reconstruction with only invariable grating, and improve the detection speed greatly which is used in the online fabric detection. And the brightness correction method is proposed to improve the detection accuracy. With the 3D reconstruction data, the disturbances brought by wrinkles, the changes of ambient light and background light or flying catkins can be identified correctly. And the correct rate of defect identification is raised. The experiment results prove that the proposed method can accurately identify fabric defects. And it can be applied to the online fabric defect detection, 3D measurement of moving object and other 3D online measurements in industry.

References

[1] Li Y., Ai J. and Sun C., Sensors **13**, 4659 (2013).

[2] Henry Y. T. Ngan and Gratham K. H. Pang, Patteren Recognition **43**, 2131 (2010).

[3] K. L. Mak, P. Peng and K F C.Yiu, Image and Vision Computing **27**, 1585 (2009).

[4] Yang Xiao-bo, Journal of Textile Research **32**, 133 (2013). (in Chinese)

[5] Xu Xiao-feng, Cotton Textile Technology **40**, 298 (2012). (in Chinese)

[6] Lucia Bissi, Giuseppe Baruffa, Pisana Placidi, Elisa Ricci, Andrea Scorzoni and Paolo Valigi, Journal of Visual Communication and Image Representation **24**, 838 (2013).

[7] Bi Mingde and Sun Zhi-zhang, Information Technology Journal **10**, 1701 (2011).

[8] Volkovas V., Eidukevičiūte M., Nogay H. S. and Akinci T. C., Mechanika **18**, 683 (2012).

[9] Hu Lu-yao, Da Peng-fei and Wang Lu-yang, Acta Optica Sinica **32**, 0212002 (2012). (in Chinese)

[10] SONG Li-Mei, ZHANG Chun-Bo, WEI Yi-Ying and CHEN Hua-Wei, Optoelectronics Letters **7**, 61 (2011).

[11] Limei Song, Changman Chen, Zhuo Chen，Jiangtao Xi and Yanguang Yu, Optoelectronics Letters **9**, 143 (2013).